NAVAL POSTGRADUATE SCHOOL
Monterey, California

THESIS

DIRECTIONAL SPREADING EFFECTS ON NONLINEAR WAVES SHOALING ON BEACHES

by

Mark C. Burton
June, 1995

Thesis Advisor: Thomas H.C. Herbers

Approved for public release; distribution is unlimited.

REPORT DOCUMENTATION PAGE

Form Approved
OMB No. 0704-0188

1. AGENCY USE ONLY (Leave Blank)	2. REPORT DATE	3. REPORT TYPE
	June, 1995	Master's Thesis

4. TITLE AND SUBTITLE
DIRECTIONAL SPREADING EFFECTS ON NONLINEAR WAVES SHOALING ON BEACHES

5. FUNDING NUMBERS

6. AUTHOR(S)
Mark C. Burton

7. PERFORMING ORGANIZATION NAMES(S) AND ADDRESS(ES)
Naval Postgraduate School
Monterey, CA 93943-5000

8. PERFORMING ORGANIZATION REPORT NUMBER

9. SPONSORING/MONITORING AGENCY NAME(S) AND ADDRESS(ES)

10. SPONSORING/MONITORING AGENCY REPORT NUMBER

11. SUPPLEMENTARY NOTES
The views expressed in this thesis are those of the author and do not reflect the official policy or position of the Department of Defense or the US Government.

12a. DISTRIBUTION/AVAILABILITY STATEMENT
Approved for public release; distribution is unlimited.

12b. DISTRIBUTION CODE

13. ABSTRACT (Maximum 200 words)

A nonlinear Boussinesq model for the shoaling of ocean surface gravity waves on beaches is presented and compared to second-order finite depth theory. The spectral Boussinesq model of Freilich and Guza (1984) for uni-directional waves propagating perpendicular to a beach with straight and parallel depth contours is extended to obliquely propagating waves. Predictions of the shoaling evolution of a single resonant triad with two primary incident wave components driving a secondary wave component are compared to finite depth theory predictions of forced secondary waves. Results for both sum- and difference-interactions are presented for a range of beach slopes, incident wave amplitudes, frequencies and propagation directions.

The comparisons show that there is a region (roughly between 10 and 4 m depth for typical swell amplitudes and frequencies) where both theories predict very similar growth of secondary wave components. Whereas Boussinesq theory typically predicts slightly smaller secondary wave amplitudes than finite depth theory, the dependence of the secondary wave response on the directional spreading angle of the primary waves predicted by both theories are in good agreement. However, pronounced discrepancies between Boussinesq and finite depth predictions are noted for very low (infragravity) frequency secondary waves on relatively steep beaches.

14. SUBJECT TERMS
Boussinesq Equations, Finite Depth Theory, Ocean Surface Gravity Waves, Nonlinear Interactions, Shoaling, Beach

15. NUMBER OF PAGES 54

16. PRICE CODE

17. SECURITY CLASSIFICATION OF REPORT	18. SECURITY CLASSIFICATION OF THIS PAGE	19. SECURITY CLASSIFICATION OF ABSTRACT	20. LIMITATION OF ABSTRACT
Unclassified	Unclassified	Unclassified	UL

NSN 7540-01-280-5500 Standard Form 298 (Rev. 2-89)

Approved for public release; distribution is unlimited.

DIRECTIONAL SPREADING EFFECTS ON NONLINEAR WAVES SHOALING ON BEACHES

Mark C. Burton
Lieutenant Commander, United States Navy
B.A., University of California, Berkeley, 1980

Submitted in partial fulfillment of the
requirements for the degree of

MASTER OF SCIENCE IN PHYSICAL OCEANOGRAPHY

from the

NAVAL POSTGRADUATE SCHOOL
June, 1995

Author: Mark C Burton
Mark C. Burton

Approved by:
T.H.C. Herbers, Thesis Advisor

T.C. Lippmann, Second Reader

Robert H Bourke
R.H. Bourke, Chairman
Department of Oceanography

ABSTRACT

A nonlinear Boussinesq model for the shoaling of ocean surface gravity waves on beaches is presented and compared to second-order finite depth theory. The spectral Boussinesq model of Freilich and Guza (1984) for uni-directional waves propagating perpendicular to a beach with straight and parallel depth contours is extended to obliquely propagating waves. Predictions of the shoaling evolution of a single resonant triad with two primary incident wave components driving a secondary wave component are compared to finite depth theory predictions of forced secondary waves. Results for both sum- and difference-interactions are presented for a range of beach slopes, incident wave amplitudes, frequencies and propagation directions.

The comparisons show that there is a region (roughly between 10 and 4 m depth for typical swell amplitudes and frequencies) where both theories predict very similar growth of secondary wave components. Whereas Boussinesq theory typically predicts slightly smaller secondary wave amplitudes than finite depth theory, the dependence of the secondary wave response on the directional spreading angle of the primary waves predicted by both theories are in good agreement. However, pronounced discrepancies between Boussinesq and finite depth predictions are noted for very low (infragravity) frequency secondary waves on relatively steep beaches.

TABLE OF CONTENTS

LIST OF SYMBOLS

a	amplitude
$a_{p,q}$	amplitude of the component p,q
$a_{p,q\,\tilde{x}}$	slow space derivative of $a_{p,q}$
$B^{(i)}$	biphase of component i
$C_{g0}^{(i)}$	deep water group velocity of component i
$C_g^{(i)}$	group velocity of component i
∇	horizontal gradient operator
$C_{\pm}$	finite depth theory coupling coefficient
ε	nonlinearity parameter
$F(t)$	arbitrary function of time
g	gravity
h	water depth
h_0	representative water depth
η	surface elevation
$\mathbf{k}_i$	(vector) wavenumber of component i
k_i	cross-shore wavenumber of component i
ℓ_q	alongshore wavenumber of component q
$\ell^{(i)}$	alongshore wavenumber of the i^{th} mode of a resonant triad
$\Delta\ell$	separation of adjacent alongshore wavenumber bands in Fourier representation
p	pressure
p_0	hydrostatic pressure of undisturbed fluid
π	pi
σ	dispersion parameter
$T_{p,q}$	slow phase evolution of component p,q
t'	scaled time
t	unscaled time
$\theta(x)$	shallow water incidence angle
θ_0	deep water incidence angle
$\mathbf{u}$	horizontal velocity vector
U_r	Ursell parameter
u_1, v_1	first order flows
$\bar{u}_2, \bar{v}_2$	depth-averaged second order flows
U_2, V_2	arbitrary horizontal velocity functions
ϕ_1	first-order velocity potential function
$\bar{\phi}_2$	depth-averaged second-order velocity potential function
$\psi_{p,q}$	phase of component p,q
w	vertical velocity

$\tilde{x}$	slow space variable
$\mathbf{x}$	horizontal position vector
x',y'	scaled horizontal coordinates
x,y	unscaled (physical) horizontal coordinates
z'	scaled vertical coordinate
z	unscaled (physical) vertical coordinate
$\omega^{(i)}$	radian frequency of the i^{th} mode of a resonant triad
ω_p	radian frequency of component p
$\Delta\omega$	separation of adjacent frequency bands in Fourier representation

ACKNOWLEDGMENT

I wish to express my sincere appreciation to my advisor, Thomas Herbers, for his guidance and for the countless hours of discussion and instruction which determined the success of this effort.

I would like also to extend my deepest gratitude to my wife, Cynthia, for supporting my work and for her encouragement and understanding.

I. INTRODUCTION

Wind-generated ocean surface gravity waves are the principal driving force for fluid motions and sediment transport in the littoral zone. Accurate models for the transformation of waves on beaches are needed to predict alongshore and rip currents, undertow, bedforms (e.g., bars and cusps) and beach erosion and accretion. In general, as waves shoal, amplitudes increase, wavelengths decrease and propagation directions change towards normal incidence to the beach. In addition to these linear shoaling and refraction effects, nonlinear wave-wave interactions cause transfers of energy to wave components with both higher and lower frequencies.

Theories for nonlinear wave-wave interactions in deep water ($kh>>1$, where k is the wavenumber and h is the water depth) and intermediate depths ($kh=O(1)$) are usually based on Stokes' (1847) perturbation expansion for weak nonlinearity ($ak<<1$, where a is the wave amplitude) (Phillips, 1960; Hasselmann, 1962; Longuet-Higgins and Stewart, 1962). A nonlinear transfer of energy to higher frequencies occurs through sum-interactions: two primary wind-waves having frequencies ω_1 and ω_2, and wavenumbers $\mathbf{k}_1$ and $\mathbf{k}_2$, excite a secondary wave, with the sum-frequency $\omega_1 + \omega_2$ and (vector) sum wavenumber $\mathbf{k}_1 + \mathbf{k}_2$. Phillips (1960) showed that at this order there are no resonances; secondary waves are forced waves that do not satisfy the gravity wave dispersion relation. Since the amplitudes are bounded, these forced waves are often called "bound waves".

The predicted forced secondary waves are phase locked to the primary wind waves, and typically distort a linear sinusoidal wave profile to shapes with peaky crests

and broad troughs. Observations of high frequency pressure and velocity fluctuations in intermediate depths agree well with second-order nonlinear theory predictions (Herbers et al., 1992; Herbers and Guza, 1991, 1992, 1994).

In shallow water, the Stokes-type perturbation solutions are valid only if the Ursell number, $Ur = \frac{a}{k^2h^3}$, is small (Stokes, 1847; Ursell, 1953). While this assumption holds well for intermediate continental shelf depths, it usually breaks down on beaches, where Ur is O(1). In this shallow region (typically h<5 m), where dispersion is weak, nonlinearities become quite significant, and asymmetrical wave shapes develop with steep forward faces.

The nonlinear shoaling region where Ur is typically O(1) is better represented by the Boussinesq equations (Boussinesq, 1871), which assume that nonlinearity $\frac{a}{h}$, and dispersion $(kh)^2$, are both weak and of the same order (i.e., Ur=O(1)). In Boussinesq theory, continuous nonlinear energy transfers take place between near-resonant wave triads. Mei and LeMéhauté (1966) and Peregrine (1967) extended the Boussinesq equations to a bottom sloping gently in 2 dimensions, and these equations have been used extensively to model the nonlinear evolution of waves shoaling on beaches.

Freilich and Guza (1984) developed a Boussinesq model for unidirectional waves propagating over a bottom varying slowly in one dimension. The predicted shoaling evolution of wave frequency spectra agrees well with field observations (Freilich and Guza, 1984; Elgar and Guza, 1985, 1986; Elgar et al., 1990). Liu, Yoon, and Kirby

(1985) developed a parabolic approximation to Peregrine's equations, allowing for small directional spreading angles on a two dimensional beach, but applications to a continuous frequency-directional spectrum of waves have not been reported.

Presently, no uniformly valid theory exists for shoaling waves. Whereas fully dispersive finite depth solutions are singular at the shoreline, weakly dispersive Boussinesq solutions break down in intermediate depths (kh=O(1)). Thus, both finite depth and Boussinesq solutions are needed to model the shoaling zone. For typical swell amplitudes (O(1 m)) and periods (O(10 s)), finite depth theory can be applied in the "outer shoaling region", extending from roughly 20-6 m depth (Herbers et al., 1992), and Boussinesq theory in the "inner shoaling region", between roughly 7 m depth and the outer edge of the breaker zone (e.g., Freilich and Guza, 1984; Elgar and Guza, 1985). Although formally the validity ranges of finite depth and Boussinesq theories do not overlap, for practical applications there is a region (roughly 5-8 m depth) where both theories are expected to be reasonably accurate. The errors in finite depth and Boussinesq model predictions in this transition region are poorly understood.

Difference-interactions between two wave components $(\omega_1,\mathbf{k}_1)$ and $(\omega_2,\mathbf{k}_2)$ excite a third wave at the difference-frequency and wavenumber, $(\omega_1-\omega_2,\mathbf{k}_1-\mathbf{k}_2)$ (for $\omega_1>\omega_2$), that typically causes a "set down" of the mean ocean surface under groups of high waves (Longuet-Higgins and Stewart, 1962). Difference-interactions are particularly important because they drive energetic nearshore low frequency motions (nominally 0.005-0.05 Hz), known as infragravity waves or "surf beat" (e.g., Munk,

1949; Tucker, 1950; Herbers et al., 1995a). Infragravity waves cause seiches in small harbors (Okihiro, et al., 1993), and are believed to be the primary means by which sediment is suspended in the inner surf zone during storms (Holman et al., 1978; Wright et al., 1982; Beach and Sternberg, 1988).

Whereas incident wind waves and the associated higher frequency secondary waves are usually dissipated in the surf-zone, the low-frequency, long-wavelength secondary waves forced by difference-interactions may reflect from shore. Longuet-Higgins and Stewart (1962) suggested that forced secondary waves at infragravity frequencies are released in the surf zone, reflect from the beach, and subsequently radiate seaward as free waves. Observations of the directional properties of infragravity waves are consistent with this mechanism (Herbers et al., 1995b), but quantitative models for the nonlinear transfer of energy to infragravity frequencies are presently lacking. Second order finite depth theory (Hasselmann, 1962, based on the Stokes expansion) predicts accurately the amplitudes of forced infragravity waves in intermediate depths (Herbers et al., 1994), but is singular near the shoreline, and thus cannot predict the amplitudes of free infragravity waves released in the surf zone (Herbers et al., 1995b). Boussinesq theory may provide quantitative estimates of free infragravity energy radiated from shore.

This paper extends the work of Freilich and Guza (1984), by examining both sum- and difference-interactions between obliquely propagating shoaling waves. The 2-dimensional Boussinesq equations for a beach with straight and parallel depth contours are derived in Chapter II, and solved for a spectrum of waves in Chapter III. The predicted evolution of amplitudes and phases for a single wave triad are compared to

predictions based on Hasselmann's (1962) second order finite depth theory in Chapter IV. The results are summarized in Chapter V. All Figures are contained in the Appendix.

II. GOVERNING EQUATIONS AND APPROXIMATIONS

In this chapter, Boussinesq equations are derived for obliquely propagating waves on a gently sloping, impermeable beach with straight and parallel depth contours. Following Peregrine (1967), non-dimensional variables will be used as follows:

$$h = \frac{h^*}{h_0} \qquad \eta = \frac{\eta^*}{h_0}$$

$$(x, y, z) = \frac{1}{h_0}(x^*, y^*, z^*) \qquad t = \sqrt{\frac{g}{h_0}}\, t^*$$

$$(u, v, w) = \frac{1}{\sqrt{g h_0}}(u^*, v^*, w^*) \qquad p = \frac{1}{\rho g h_0}\, p^*$$

where * indicates a dimensional variable and h_0 is a representative water depth. The z axis points vertically upwards, with z=0 corresponding to the mean surface. The x axis points onshore, and y points alongshore (Figure 1). The variables p, u, v, and w denote pressure and the velocity components in the x, y, and z directions, respectively. The free surface is defined by $z = \eta(\mathbf{x}, t)$ where $\mathbf{x}$ is the horizontal space vector (x,y). The bottom is defined by $z = -h(x)$.

The equations of motion and the continuity equation in non-dimensionalized form (neglecting viscous effects) are:

$$\frac{\partial \mathbf{u}}{\partial t} + (\mathbf{u} \cdot \nabla)\mathbf{u} + w\frac{\partial \mathbf{u}}{\partial z} + \nabla p = 0 \qquad (2\text{-}1)$$

$$\frac{\partial w}{\partial t} + (\mathbf{u} \cdot \nabla) w + w \frac{\partial w}{\partial z} + \frac{\partial p}{\partial z} + 1 = 0 \tag{2-2}$$

$$\nabla \cdot \mathbf{u} + \frac{\partial w}{\partial z} = 0 \tag{2-3}$$

where ∇ denotes the two dimensional gradient operator $\left(\frac{\partial}{\partial x}, \frac{\partial}{\partial y}\right)$, and $\mathbf{u}$ indicates the horizontal velocity vector (u, v). The surface and bottom boundary conditions are given by

$$w = \frac{\partial \eta}{\partial t} + \mathbf{u} \cdot \nabla \eta \qquad \text{at} \quad z = \eta(\mathbf{x}, t) \tag{2-4a}$$

$$p = 0 \qquad \text{at} \quad z = \eta(\mathbf{x}, t) \tag{2-4b}$$

$$w = -u \frac{\partial h}{\partial x} \qquad \text{at} \quad z = -h(x) \tag{2-4c}$$

Irrotational flow is assumed, which yields the relation:

$$\frac{\partial \mathbf{u}}{\partial z} = \nabla w \tag{2-5}$$

The continuity Equation (2-3) can be vertically integrated using the kinematic boundary conditions (2-4a,c) and Leibniz's Theorem:

$$\nabla \cdot \int_{-h}^{\eta} \mathbf{u} dz + \frac{\partial \eta}{\partial t} = 0 \tag{2-6}$$

Following Peregrine (1967), the variables η, p, and **u** are expanded in terms of the non-linearity parameter ε, defined to be the ratio of wave amplitude to water depth $\varepsilon = a/h$,

$$\begin{aligned} \eta &= \varepsilon\eta_1 + \varepsilon^2\eta_2 + \ldots \\ p &= p_0 + \varepsilon p_1 + \varepsilon^2 p_2 + \ldots \\ \mathbf{u} &= \varepsilon\mathbf{u}_1 + \varepsilon^2\mathbf{u}_2 + \ldots \end{aligned} \tag{2-7}$$

where $p_0 = -z$, is the hydrostatic pressure of the undisturbed fluid. In shallow water, the vertical velocity component w is $O(\sigma)$ smaller than **u**, where the dispersion parameter, $\sigma = kh$, is the product of the wavenumber and the water depth:

$$w = \sigma\left(\varepsilon w_1 + \varepsilon^2 w_2 + \ldots\right) \tag{2-8}$$

Even waves with a large oblique incidence angle θ_0 relative to the shore-normal in deep water will refract so that the angle, $\theta(x)$, in shallow water is small and thus $v << u$. Assuming that the waves incident from deep water propagate over a seabed with approximately straight and parallel depth contours, the scaling of the v component follows from Snell's law:

$$\sin(\theta(x)) = \frac{\omega^2}{|k(x)|}\sin\theta_0$$

where ω and $\mathbf{k}(x)=(k(x),\ell)$ are the non-dimensionalized wave frequency and wavenumber vector. In shallow water this relation reduces to

$$\theta(x) \approx k(x)h(x)\sin\theta_0 \tag{2-9}$$

Hence, the ratio between v and u in shallow water is $O(kh)$, and we can write:

$$\begin{aligned} u &= \varepsilon u_1 + \varepsilon^2 u_2 + \ldots \\ v &= \sigma\left(\varepsilon v_1 + \varepsilon^2 v_2 + \ldots\right) \end{aligned} \tag{2-10}$$

The independent variables are scaled accordingly:

$$\frac{\partial}{\partial x} = \sigma\frac{\partial}{\partial x'} \quad , \quad \frac{\partial}{\partial y} = \sigma^2\frac{\partial}{\partial y'} \quad , \quad \frac{\partial}{\partial z} = \frac{\partial}{\partial z'} \quad , \quad \frac{\partial}{\partial t} = \sigma\frac{\partial}{\partial t'} \tag{2-11}$$

Since the variables $\eta_i, p_i, \mathbf{u}_i$ and w_i $(i = 0,1,\ldots)$ are $O(1)$, the order of the terms appears explicitly when the relations (2-7), (2-8), (2-10) and (2-11) are substituted into the governing equations.

The water depth h is assumed to be a slow function of x'.

$$h = h(\tilde{x}) \tag{2-12}$$

where $\tilde{x} = \varepsilon x'$ is a slow space variable, so that

$$\frac{\partial h}{\partial x'} = \varepsilon\frac{\partial h}{\partial \tilde{x}} \tag{2-13}$$

Note that in dimensional coordinates, the beach slope $\frac{\partial h^*}{\partial x^*}$ is $O(\sigma\varepsilon)$. Thus, for typical shoaling wave values of $\varepsilon = 0.05, \sigma = 0.2$, the beach slope is assumed to be $O(10^{-2})$. This is a realistic slope for a natural sandy beach.

First order relations for the wave-induced velocity and pressure fields are obtained by substituting Equations (2-7), (2-8), (2-10) and (2-11) into Equations (2-2) and (2-5)

$$\frac{\partial u_1}{\partial z'} = O(\varepsilon) \tag{2-14a}$$

$$\frac{\partial v_1}{\partial z'} = O(\varepsilon) \tag{2-14b}$$

$$\frac{\partial p_1}{\partial z'} = O(\varepsilon) \tag{2-14c}$$

It follows from Equation (2-14) that u_1, v_1, and p_1 are independent of z'. Equation 2-14c integrates to (using the dynamic free surface boundary condition (Equation (2-4b))):

$$p_1 = \eta_1 \tag{2-15}$$

The first order horizontal momentum equations can be obtained by substituting Equations (2-7), (2-8), (2-10), (2-11), and (2-15) into Equation (2-1). In component form:

$$\frac{\partial u_1}{\partial t'} + \frac{\partial \eta_1}{\partial x'} = O(\varepsilon) \tag{2-16a}$$

$$\frac{\partial v_1}{\partial t'} + \frac{\partial \eta_1}{\partial y'} = O(\varepsilon) \tag{2-16b}$$

Similarly, substituting Equations (2-7), (2-10), (2,11), and (2-13) in Equation (2-6) yields the first order depth-integrated continuity equation:

$$\frac{\partial \eta_1}{\partial t'} + h\frac{\partial u_1}{\partial x'} = O(\varepsilon) \tag{2-17}$$

Substituting Equations (2-7), (2-8), (2-10), and (2-11) in Equations (2-2) and (2-5) we obtain the second order relations

$$\frac{\partial u_2}{\partial z'} = \frac{\partial w_1}{\partial x'} + O(\varepsilon) \tag{2-18a}$$

$$\frac{\partial v_2}{\partial z'} = \frac{\partial w_1}{\partial y'} + O(\varepsilon) \tag{2-18b}$$

$$\frac{\partial p_2}{\partial z'} = -\frac{\partial w_1}{\partial t'} + O(\varepsilon) \tag{2-18c}$$

Vertically integrating the first order continuity equation (Equations (2-3), (2-10), (2-11)):

$$\frac{\partial u_1}{\partial x'} + \frac{\partial w_1}{\partial z'} = O(\varepsilon)$$

using Equations (2-4c), and (2-13) yields

$$w_1(z') = -(z' + h)\frac{\partial u_1}{\partial x'} + O(\varepsilon) \tag{2-19}$$

Substitution of Equation (2-19) in Equation (2-18a-c) and integration with respect to z' (using the dynamic free surface boundary condition (Equation 2-4b)) yields:

$$u_2 = U_2(x',y',t') - \left[z'h + \frac{z'^2}{2} \right] \frac{\partial^2 u_1}{\partial x' \partial y'} + O(\varepsilon) \qquad (2\text{-}20a)$$

$$v_2 = V_2(x',y',t') - \left[z'h + \frac{z'^2}{2} \right] \frac{\partial^2 u_1}{\partial x' \partial y'} + O(\varepsilon) \qquad (2\text{-}20b)$$

$$p_2 = \eta_2(x',y',t') + \left[z'h + \frac{z'^2}{2} \right] \frac{\partial^2 u_1}{\partial x' \partial y'} + O(\varepsilon) \qquad (2\text{-}20c)$$

where U_2 and V_2 are arbitrary velocity functions arising from the integration. These functions can be expressed in terms of the depth averaged second order flows $\bar{u}_2$ and $\bar{v}_2$ by vertically integrating Equations (2-20a,b):

$$\bar{u}_2 \equiv \frac{1}{h+\eta} \int_{-h}^{\eta} u_2 dz' = U_2(x',y',t') + \frac{1}{3} h^2 \frac{\partial^2 u_1}{\partial x'^2} + O(\varepsilon) \qquad (2\text{-}21a)$$

$$\bar{v}_2 \equiv \frac{1}{h+\eta} \int_{-h}^{\eta} v_2 dz' = V_2(x',y',t') + \frac{1}{3} h^2 \frac{\partial^2 u_1}{\partial x' \partial y'} + O(\varepsilon) \qquad (2\text{-}21b)$$

Finally, substituting the perturbation expansions (2-7), (2-8), (2-10), and (2-11), the first order relation (2-15) and the second-order relations (2-20a,b,c) and (2-21a,b) back into the horizontal momentum Equation (2-1) yields, componentwise:

$$\frac{\partial \eta_1}{\partial x'} + \frac{\partial u_1}{\partial t'} + \varepsilon \left(\frac{\partial \eta_2}{\partial x'} + \frac{\partial \bar{u}_2}{\partial t'} + u_1 \frac{\partial u_1}{\partial x'} - \frac{1}{3} h^2 \frac{\partial^3 u_1}{\partial x'^2 \partial t'} \right) = O(\varepsilon^2) \qquad (2\text{-}22a)$$

$$\frac{\partial \eta_1}{\partial y'} + \frac{\partial v_1}{\partial t'} + \varepsilon \left(\frac{\partial \eta_2}{\partial y'} + \frac{\partial \overline{v}_2}{\partial t'} + u_1 \frac{\partial v_1}{\partial x'} - \frac{1}{3} h^2 \frac{\partial^3 u_1}{\partial x' \partial y' \partial t'} \right) = O(\varepsilon^2) \qquad (2\text{-}22b)$$

and the corresponding second-order depth-integrated continuity equation is obtained by substituting Equations (2-7), (2-10), (2-11), and (2-13) into Equation (2-6):

$$\frac{\partial \eta_1}{\partial t'} + \frac{\partial u_1}{\partial x'} + \varepsilon \left(\frac{\partial \eta_2}{\partial t'} + h \frac{\partial \overline{u}_2}{\partial x'} + h \frac{\partial v_1}{\partial y'} + \frac{\partial}{\partial x'} (\eta_1 u_1) + u_1 \frac{\partial h}{\partial \widetilde{x}} \right) = O(\varepsilon^2) \qquad (2\text{-}22c)$$

III. SPECTRAL SOLUTIONS

In Chapter II, an approximate set of governing equations was derived (2-22a,b,c) for waves shoaling on a beach with straight and parallel depth contours. In this chapter, these equations will be solved for a frequency-directional spectrum of waves. Equations (2-22a,b,c) can be expressed in terms of the first- and (depth-averaged) second-order velocity potential functions ϕ_1 and $\bar{\phi}_2$:

$$u_1 = \frac{\partial \phi_1}{\partial x'} \quad ; \; v_1 = \frac{\partial \phi_1}{\partial y'}$$

$$\bar{u}_2 = \frac{\partial \bar{\phi}_2}{\partial x'} + O(\varepsilon); \; \bar{v}_2 = \frac{\partial \bar{\phi}_2}{\partial y'} + O(\varepsilon)$$

Dropping the primes to simplify the notation:

$$\eta_{1x} + \phi_{1xt} + \varepsilon\left(\eta_{2x} + \bar{\phi}_{2xt} + \phi_{1x}\phi_{1xx} - \frac{1}{3}h^2\phi_{1xxxt} \right) = O(\varepsilon^2) \tag{3-1a}$$

$$\eta_{1y} + \phi_{1yt} + \varepsilon\left(\eta_{2y} + \bar{\phi}_{2yt} + \phi_{1x}\phi_{1xy} - \frac{1}{3}h^2\phi_{1xxyt} \right) = O(\varepsilon^2) \tag{3-1b}$$

$$\eta_{1t} + h\phi_{1xx} + \varepsilon\left(\eta_{2t} + h\bar{\phi}_{2xx} + h\phi_{1yy} + \left(\eta_1\phi_{1x}\right)_x + \phi_{1x}h_{\tilde{x}} \right) = O(\varepsilon^2) \tag{3-1c}$$

where subscripts t, x, y, $\tilde{x}$ indicate derivatives.

The lowest order wave field (η_1, ϕ_1) is assumed to be a linear superposition of nearly plane, shoreward propagating waves with frequency ω_p and alongshore wavenumber ℓ_q.

$$\eta_1 = \sum_{p=-\infty}^{\infty} \sum_{q=-\infty}^{\infty} \frac{1}{2} a_{p,q}(\tilde{x}) \exp\left[i(\psi_{p,q}(x) + \ell_q y - \omega_p t)\right]$$
$$\phi_1 = \sum_{p=-\infty}^{\infty} \sum_{q=-\infty}^{\infty} \frac{1}{2i\omega_p} a_{p,q}(\tilde{x}) \exp\left[i(\psi_{p,q}(x) + \ell_q y - \omega_p t)\right] \qquad (3\text{-}2)$$

where $\omega_p = p\Delta\omega$ and $\ell_q = q\Delta\ell$, with $\Delta\omega$ and $\Delta\ell$ the separation of adjacent bands in the Fourier representation, and the spatial variation in phase is given by

$$\frac{\partial \psi_{p,q}}{\partial x} = \frac{\omega_p}{\sqrt{h(\tilde{x})}} + \varepsilon T_{p,q}(\tilde{x}) \qquad (3\text{-}3)$$

The amplitude ($a_{p,q}$) and phase ($\psi_{p,q}$) functions include a slow variation with x, owing to shoaling, refraction and non-linear effects. This same slow space variable $\tilde{x}$ was used previously to scale the beach slope in Equations (2-12) and (2-13). In order for η_1 and ϕ_1 to be real requires:

$$a_{p,q} = a_{-p,-q} \qquad \psi_{p,q} = -\psi_{-p,-q} \qquad T_{p,q} = -T_{-p,-q}$$

Linear terms involving η_2 are eliminated from the governing Equations (3-1a,b,c) by cross differentiating ($\frac{\partial}{\partial t}$ (3-1a) - $\frac{\partial}{\partial x}$ (3-1c) and $\frac{\partial}{\partial t}$ (3-1b) - $\frac{\partial}{\partial y}$ (3-1c)):

$$\phi_{1xtt} - (h\phi_{1xx})_x + \varepsilon\left(\overline{\phi}_{2xtt} - (h\overline{\phi}_{2xx})_x + (\phi_{1x}\phi_{1xx})_t - \frac{1}{3}h^2\phi_{1xxxtt} - (h\phi_{1yy})_x - (\eta_1\phi_{1x})_{xx} - (h_{\tilde{x}}\phi_{1x})_x\right) = O(\varepsilon^2) \qquad (3\text{-}4)$$

$$\phi_{1ytt} - (h\phi_{1xx})_y + \varepsilon\left(\overline{\phi}_{2ytt} - (h\overline{\phi}_{2xx})_y + (\phi_{1x}\phi_{1xy})_t - \frac{1}{3}h^2\phi_{1xxytt} - (h\phi_{1yy})_y - (\eta_1\phi_{1x})_{xy} - (h_{\tilde{x}}\phi_{1x})_y\right) = O(\varepsilon^2) \qquad (3\text{-}5)$$

Equations (3-4) and (3-5) can be expressed as:

$$\nabla\left\{\phi_{1tt} - h\phi_{1xx} + \varepsilon\left(\overline{\phi}_{2tt} - h\overline{\phi}_{2xx} + \frac{1}{2}(\phi_{1x}^2)_t - \frac{1}{3}h^2\phi_{1xxtt} - h\phi_{1yy} - (\eta_1\phi_{1x})_x - h_{\tilde{x}}\phi_{1x}\right)\right\} = O(\varepsilon^2)$$

(3-6)

(with ∇ the (scaled) horizontal gradient operator $\nabla \equiv \left(\frac{\partial}{\partial x}, \frac{\partial}{\partial y}\right)$), which integrates to

$$\phi_{1tt} - h\phi_{1xx} + \varepsilon\left(\overline{\phi}_{2tt} - h\overline{\phi}_{2xx} + \frac{1}{2}(\phi_{1x}^2)_t - \frac{1}{3}h^2\phi_{1xxtt} - h\phi_{1yy} - (\eta_1\phi_{1x})_x - h_{\tilde{x}}\phi_{1x}\right) = F(t) + O(\varepsilon^2)$$

(3-7)

where F(t) is an arbitrary function of time arising from the integration which we set equal to zero. Substitution of the lowest order wave field (Equation (3-2) and (3-3)) into Equation (3-7) yields, after some algebraic manipulations:

$$\phi_{2tt} - h\phi_{2xx} = \sum_{p=-\infty}^{\infty}\sum_{q=-\infty}^{\infty}\left\{\frac{1}{4}a_{p,q}\frac{h_{\tilde{x}}}{\sqrt{h}} + a_{p,q\tilde{x}}\sqrt{h} + i\left(a_{p,q}\sqrt{h}T_{p,q} - \frac{1}{6}a_{p,q}h\omega_p^3 + \frac{1}{2}a_{p,q}\frac{h}{\omega_p}\ell_q^2\right)\right.$$
$$\left. + i\frac{3}{8h}\sum_{m=-\infty}^{\infty}\sum_{n=-\infty}^{\infty}a_{p-m,m-n}a_{m,n}\omega_p\exp\left[i\left(\psi_{p-m,q-n} + \psi_{m,n} - \psi_{p,q}\right)\right]\right\}\exp\left[i\left(\psi_{p,q}(x) + \ell_q y - \omega_p t\right)\right] + O(\varepsilon) \quad (3\text{-}8)$$

The left-hand side of Equation (3-8) is the wave equation for $\overline{\phi}_2$. To prevent resonant growth of $\overline{\phi}_2$ (which would upset the perturbation expansion, Equation (2-7)) requires that the forcing terms on the right-hand side of Equation (3-8) do not contain any free oscillations. Since all these terms obey the lowest-order dispersion relation (Equation (3-3)), it follows that the right-hand side of Equation (3-8) must vanish.

Collecting like frequencies and alongshore wavenumbers and solving for the real and imaginary parts yields a coupled set of equations for the amplitude and phase evolution of the lowest order waves:

$$a_{p,q\tilde{x}} = -\frac{1}{4} a_{p,q} \frac{h_{\tilde{x}}}{h} + \frac{3}{8} h^{-\frac{3}{2}} \omega_p \sum_{m=-\infty}^{\infty} \sum_{n=-\infty}^{\infty} a_{p-m,q-n} a_{m,n} \sin\left(\psi_{p-m,q-n} + \psi_{m,n} - \psi_{p,q}\right) \qquad (3\text{-}9a)$$

$$T_{p,q} = \frac{1}{6} \sqrt{h}\, \omega_p^3 - \frac{\sqrt{h}}{2\omega_p} \ell_q^{\,2} - \frac{3}{8a_{p,q}} h^{-\frac{3}{2}} \omega_p \sum_{m=-\infty}^{\infty} \sum_{n=-\infty}^{\infty} a_{p-m,q-n} a_{m,n} \cos\left(\psi_{p-m,q-n} + \psi_{m,n} - \psi_{p,q}\right) \qquad (3\text{-}9b)$$

The first term on the right hand side of Equation (3-9a) is the amplitude growth of the mode due to shoaling. The first and second terms on the right hand side of Equation (3-9b) are dispersion and refraction corrections to the wave phase. The double summation terms give the amplitude growth and phase changes of a mode due to resonant non-linear interactions of all possible triads in which the mode participates. For uni-directional, normally incident waves, Equations (3-9a,b) reduce to Freilich and Guza's (1984) "consistent shoaling model" (Equations (16a,b) in their paper).

Finally, we re-dimensionalize Equations (3-9a,b), and re-express them in unscaled (physical) coordinates. Dropping the "*" used previously to denote dimensional coordinates, and using Equation (3-3), we obtain

$$a_{p,qx} = -\frac{1}{4} a_{p,q} \frac{h_x}{h} + \frac{3}{8} h^{-\frac{3}{2}} \frac{\omega_p}{\sqrt{g}} \sum_{m=-\infty}^{\infty} \sum_{n=-\infty}^{\infty} a_{p-m,q-n} a_{m,n} \sin\left(\psi_{p-m,q-n} + \psi_{m,n} - \psi_{p,q}\right) \qquad (3\text{-}10a)$$

$$\Psi_{p.qx} = \frac{\omega_p}{\sqrt{gh}} + \frac{1}{6}\sqrt{h}\left(\frac{\omega_p}{\sqrt{g}}\right)^3 - \frac{\sqrt{gh}}{2\omega_p}\ell_q^2 - \frac{3}{8a_{p,q}}h^{-\frac{3}{2}}\frac{\omega_p}{\sqrt{g}}\sum_{m=-\infty}^{\infty}\sum_{n=-\infty}^{\infty} a_{p-m,q-n}a_{m,n}\cos\left(\psi_{p-m,q-n} + \psi_{m,n} - \psi_{p,q}\right)$$

(3-10b)

IV. COMPARISON TO FINITE DEPTH THEORY

In this Chapter the amplitude and phase evolution given by Equation (3-10a,b) are compared to predictions of second-order nonlinear finite depth theory (Hasselmann, 1962). The Boussinesq equations were integrated over a plane beach for a single resonant triad consisting of two primary waves incident from deep water that drive a secondary wave component. Both sum- and difference-interactions are compared for a range of commonly observed beach slopes, incident wave amplitudes, frequencies, and propagation directions. The objective of these comparisons is to examine the similarities and differences of Boussinesq and finite depth theory predictions in the transition region from deep to shallow water, and in particular to investigate the dependence of the secondary wave growth on the directional spreading angle of the primary waves. While this approach is useful to describe the initial growth of a secondary wave component, in very shallow water the secondary wave amplitude grows to become comparable to the primary wave amplitudes and thus fully coupled spectral calculations are needed to predict the nonlinear shoaling evolution.

For a single triad, we can simplify the notation used in Equation (3-10a,b) by introducing a single index i=1,2,3, where mode i has a frequency $\omega^{(i)}$ ($0 < \omega^{(1)} < \omega^{(2)} < \omega^{(3)}$), alongshore wavenumber $\ell^{(i)}$, amplitude $a^{(i)}$, and phase $\psi^{(i)}$, and the triad satisfies the resonance rule:

$$\omega^{(3)} = \omega^{(1)} + \omega^{(2)} \quad , \quad \ell^{(3)} = \ell^{(1)} + \ell^{(2)}$$

The amplitude and phase evolution equations for this triad can be expressed (neglecting energy exchanges with any other components) compactly as:

$$a_x^{(i)} = S^{(i)} + N^{(i)} \sin B^{(i)} \tag{4-1a}$$

$$\psi_x^{(i)} = k^{(i)} + D^{(i)} + R^{(i)} - \frac{N^{(i)}}{a^{(i)}} \cos B^{(i)} \tag{4-1b}$$

with:

$$S^{(i)} = -\frac{1}{4} a^{(i)} \frac{h_x}{h} \qquad \text{(shoaling term)}$$

$$k^{(i)} = \frac{\omega^{(i)}}{\sqrt{gh}} \qquad \text{(shallow water wave number)}$$

$$D^{(i)} = \frac{1}{6} \sqrt{h} \left(\frac{\omega^{(i)}}{\sqrt{g}} \right)^3 \qquad \text{(dispersion term)}$$

$$R^{(i)} = -\frac{\sqrt{gh}}{2\omega^{(i)}} \ell^{(i)2} \qquad \text{(refraction term)}$$

$$N^{(i)} = \frac{3}{4} h^{-3/2} \frac{\omega^{(i)}}{\sqrt{g}} a^{(n)} a^{(m)} \qquad \text{(nonlinear interaction term)}$$

$$-B^{(1)} = -B^{(2)} = B^{(3)} = \psi^{(1)} + \psi^{(2)} - \psi^{(3)} \qquad \text{(biphase)}$$

A first-order finite difference scheme using an Arakawa A grid with a step size of 0.1 m was used to integrate Equation (4-1). Test runs with grid spacings of 0.01 m and 1.0 m yielded identical results, confirming the accuracy of the numerical scheme. Additional tests of the numerical scheme include a verification of energy conservation.

In second-order finite depth theory, two primary waves with frequencies $\omega^{(1)}$ and $\omega^{(2)}$ ($\omega^{(1)} > \omega^{(2)} > 0$) and alongshore wavenumbers $\ell^{(1)}$ and $\ell^{(2)}$ excite secondary wave components with the sum-frequency and wavenumber ($\omega^{(1)} + \omega^{(2)}$, $\ell^{(1)} + \ell^{(2)}$), and the difference-frequency and wave number ($\omega^{(1)} - \omega^{(2)}$, $\ell^{(1)} - \ell^{(2)}$). In finite depth theory, the free surface elevation is given by

$$\begin{aligned}\eta(x,y,t) &= a^{(1)}\cos(\psi^{(1)}(x)+\ell^{(1)}y-\omega^{(1)}t)+a^{(2)}\cos(\psi^{(2)}(x)+\ell^{(2)}y-\omega^{(2)}t)\\ &+C_{+}a^{(1)}(x)a^{(2)}(x)\cos\left(\psi^{(1)}(x)+\psi^{(2)}(x)+\left[\ell^{(1)}+\ell^{(2)}\right]y-\left[\omega^{(1)}+\omega^{(2)}\right]t\right)\\ &+C_{-}a^{(1)}(x)a^{(2)}(x)\cos\left(\psi^{(1)}(x)-\psi^{(2)}(x)+\left[\ell^{(1)}-\ell^{(2)}\right]y-\left[\omega^{(1)}-\omega^{(2)}\right]t\right)\\ &+\text{other second-order terms}\end{aligned} \tag{4-2}$$

where the primary wave amplitudes $a^{(1)}$, $a^{(2)}$ and phases $\psi^{(1)}$, $\psi^{(2)}$ are given by the linear shoaling and refraction relations:

$$a^{(i)}(x) = \left[\frac{C_{go}^{(i)}\cos\theta_o^{(i)}}{C_g^{(i)}(x)\cos\left(\theta^{(i)}(x)\right)}\right]^{1/2} a_o^{(i)} \quad ; \quad \psi^{(i)}(x) = \psi_o^{(i)} + \int_o^x k^{(i)}(\zeta)d\zeta \quad ; \quad i = 1,2 \tag{4-3}$$

with subscripts o indicating deep water values at x = 0. C_g denotes the group velocity and $\theta^{(i)}$ is given by Snell's law. The coupling coefficients C_+ and C_- for the sum- and difference-interactions are given by (Hasselmann, 1962):

$$C_{\pm} = \frac{\left(\omega^{(1)} \pm \omega^{(2)}\right)^2}{g\left|\mathbf{k}^{(1)} \pm \mathbf{k}^{(2)}\right| \tanh\left(\left|\mathbf{k}^{(1)} \pm \mathbf{k}^{(2)}\right| h\right) - \left(\omega^{(1)} \pm \omega^{(2)}\right)^2}$$

$$x\left\{\pm\frac{\omega^{(1)}\omega^{(2)}}{g} - \frac{g\mathbf{k}^{(1)} \cdot \mathbf{k}^{(2)}}{\omega^{(1)}\omega^{(2)}} - \frac{g}{2\left(\omega^{(1)} \pm \omega^{(2)}\right)}\left(\frac{\left|\mathbf{k}^{(1)}\right|^2}{\omega^{(1)} \cosh^2\left(\left|\mathbf{k}^{(1)}\right| h\right)} \pm \frac{\left|\mathbf{k}^{(2)}\right|^2}{\omega^{(2)} \cosh^2\left(\left|\mathbf{k}^{(2)}\right| h\right)}\right)\right\} \quad (4\text{-}4)$$
$$+ \frac{\omega^{(1)^2} \pm \omega^{(1)}\omega^{(2)} + \omega^{(2)^2}}{2g} - \frac{g\mathbf{k}^{(1)} \cdot \mathbf{k}^{(2)}}{2\omega^{(1)}\omega^{(2)}}$$

with $\mathbf{k}^{(i)}$ the vector wavenumber of component i ($k^{(i)}(x)$, $\ell^{(i)}$).

Finite depth theory predictions of primary and secondary wave amplitudes in 10 m depth were used to initialize the Boussinesq model (Equation (4-1)). The biphase B in Equation (4-1) was matched to the finite depth value (0 or π, depending on the sign of $C_{\pm}$, Equations (4-2), (4-4)).

Boussinesq and finite depth theory predictions of sum- and difference-frequency waves forced by a pair of swell components with frequencies 0.08 and 0.12 Hz on a slope 0.01 beach are compared in Figures 2 and 3. The deep water incident wave amplitudes in these simulations are 0.2 m. In Figure 2 results are shown for two normally incident swell components. In Figure 3 the 0.08 Hz component is normally incident while the 0.12 Hz component has a deep water incidence angle of 60°. In all cases the Boussinesq and finite depth theory predictions show very similar secondary wave growth between 10 and 4 m depth. Overall, the amplitudes predicted by finite depth theory are slightly higher than those predicted by Boussinesq theory, suggesting that finite depth theory overpredicts the secondary wave growth when the triad is close to resonance. Boussinesq

theory predictions of the biphase are generally close to the finite depth theory values of 0 (sum-interactions) and π (difference-interactions). The secondary wave amplitude growth in the Boussinesq predictions is controlled by the biphase of the triad (Equation (4-12)). The growth vanishes when B is equal to the finite depth values of 0 or π. Hence, the Boussinesq and finite depth theories do not smoothly match in 10 m depth and the Boussinesq biphase appears to oscillate around, and converge to the small value which causes the secondary wave to grow at the same rate as predicted by finite depth theory.

The amplitude and biphase discrepancies between Boussinesq and finite depth theory predictions are generally larger for difference-interactions than for sum-interactions (Figures 2, 3 and other examples discussed below). Errors are expected in both finite depth and Boussinesq theory predictions for triads involving a low (infragravity) frequency secondary wave component because the infragravity wavelengths are much longer than those of the incident swell. For example, in the model run shown in Figure (2a,c) the wavelength of the 0.04 Hz difference-frequency component varies between 250 and 150 m and thus the depth variations over a wavelength (1.5 to 2.5 m) are appreciable.

While the predicted sum-frequency secondary wave amplitudes are only slightly smaller for obliquely propagating primary waves than for normally incident primary waves (cf. Figures 2b and 3b), the 60° angular separation of the primary waves causes about an order of magnitude reduction in the difference-frequency secondary wave amplitude (cf. Figures 2a and 3a). The dependence of the sum- and difference-frequency secondary wave amplitudes on primary wave incidence angles is illustrated in Figures 4-

6. Secondary wave amplitudes in 4 m depth, normalized by the product of the primary wave amplitudes (in the same depth), are shown versus the directional spreading angle of the primary waves in deep water for a range of beach slopes and primary wave frequencies and amplitudes. In finite depth theory the normalized amplitude is equal to the coupling coefficient C (Equation (4-2)) and thus can be interpreted as the secondary wave response.

In Figure 4 results are shown for primary wave pairs with frequencies (0.09 Hz, 0.11 Hz) and (0.07 Hz, 0.13 Hz), and amplitudes 0.2 m on a slope 0.01 beach. In Figure 5 the response of a (0.08 Hz, 0.12 Hz) primary wave pair with amplitudes 0.1 m is compared to the response of the same frequency pair, but with larger amplitudes 0.4 m, on a slope 0.01 beach. Results for 0.2 m amplitude primary waves with frequencies (0.08 Hz, 0.12 Hz) on two different beach slopes 0.003 and 0.03 are shown in Figure 6. The Boussinesq and finite depth theory predictions of the dependence of the secondary wave response on the directional spreading angle of the two primary waves are generally in good agreement. In all cases sum-interactions are insensitive to the spreading angle with approximately a 10-20% decrease in the response when the spreading angle increases from 0 to 60°. The magnitude of the predicted sum-frequency response is insensitive to the primary wave frequencies and the beach slope with Boussinesq predictions consistently about 25% lower than finite depth predictions (cf. Figures 4b,d; 6b,d). However, while Boussinesq predictions of the sum-frequency response for 0.1 m amplitude primary waves (Figure 5b), are in very close agreement (about 10-20% lower) with the finite depth values, the Boussinesq predictions for 0.4 m amplitude waves are

about 30-50% lower than the finite depth values (Figure 5d). In this case finite depth theory predicts secondary wave amplitudes that are comparable to primary wave amplitudes and thus is not valid. Boussinesq theory predicts a reduced response for these large amplitude primary waves that is virtually independent of the spreading angle.

The difference-frequency secondary wave response is much more sensitive to the directional spreading angle than the sum-frequency response (cf. Figures 4a,c; 5a,c; 6a,c to Figures 4b,d; 5b,d; 6b,d). An increase in deep water spreading angle from 0 to 60° causes a reduction in the difference-frequency response by a factor 3 to 10. The Boussinesq predictions are generally in good agreement with finite depth theory predictions, showing somewhat lower response levels but approximately the same variation with directional spreading angle. However, the agreement is much better on a gentle (0.003) slope (Figure 6a) than on a steep (0.03) slope (Figure 6c). In the latter case the depth changes from 10 to 4 m over a distance comparable to the secondary wavelength and the small beach slope assumption used in both Boussinesq and finite depth theory is grossly violated. Similar, but less pronounced discrepancies, between the Boussinesq and finite depth theory predictions for 0.02 Hz secondary waves (Figure 4a, with wavelengths 0(500 m)) suggests a break down of the small beach slope approximation.

Overall, the comparisons of Boussinesq and finite depth theory predictions of secondary wave growth in the transition region from deep to shallow water show surprisingly good agreement. The Boussinesq predictions of both sum- and difference-frequency secondary wave amplitudes are slightly lower than finite depth predictions but

the dependence on directional spreading angle predicted by both theories are in excellent agreement.

V. CONCLUSIONS

Although wave transformation on beaches is generally well described by one-dimensional models, the directionality of waves is of crucial importance to a variety of nearshore processes including infragravity waves, longshore currents and sediment transport. In this paper Freilich and Guza's (1984) one-dimensional spectral model for the shoaling of uni-directional waves on a beach, based on the Boussinesq equations for weakly nonlinear, weakly dispersive waves in slowly varying depth (Peregrine, 1967) is extended to two dimensions. A beach with straight and parallel depth contours is assumed on which wave incidence angles are reduced by refraction. In this approximation, dispersion and directional spreading effects are shown to be of the same order, and near-resonant nonlinear interactions occur between any pair of incident wave components. A two-dimensional Fourier representation in the frequency and alongshore wavenumber domain is used to describe the lowest order wave field, yielding a coupled set of equations for the amplitude and phase evolution of each Fourier mode. For uni-directional waves these equations reduce to Freilich and Guza's model.

Model results for the simple case of a single triad of waves are compared to second-order nonlinear, fully dispersive finite depth theory (Hasselmann, 1962) for a typical range of beach slopes and swell amplitudes, frequencies and propagation directions. In these model runs two primary swell components force a third (secondary) wave component with the sum- or difference-frequency and alongshore wavenumber. The Boussinesq model (not valid in deep water) was initialized using the finite depth theory predictions of the amplitudes and biphase in 10 m depth. Boussinesq and finite

depth theory predictions of both sum- and difference-interations are compared in the transition region from deep to shallow water (10-4 m depth) where both theories are expected to be reasonably accurate.

In general, both theories predict very similar secondary wave amplitude growth, with Boussinesq predictions typically slightly lower than finite depth predictions. The dependence of the secondary wave response on the directional spreading angle of the incident swell components in deep water predicted by both theories are in excellent agreement. Whereas the sum-frequency response is only slightly reduced for large spreading angles, difference-interactions are sensitive to the primary wave directions with typical reductions in secondary wave amplitudes of a factor of 3 to 10 when the primary wave spreading angle increases from 0° to 60°.

Not surprising, discrepancies between Boussinesq and finite depth theory are most pronounced for low (infragravity) frequency secondary waves on a relatively steep beach. In this case depth variations are appreciable over distances comparable to the secondary wavelength and the small beach slope assumption used in both theories is violated.

APPENDIX

Figure 1. Definitional sketch of variables and coordinate frame. Obliquely propagating waves shoal upon a beach having straight and parallel depth contours. h_0 is a representative water depth in the region, θ is the wave propagation angle, and **k** is the wavenumber vector.

Figure 2. Comparisons of Boussinesq and finite depth theory predictions of the shoaling evolution of a single wave triad. A pair of normally incident primary swell components with frequencies 0.08 Hz and 0.12 Hz drives a difference-frequency (0.04 Hz) secondary wave (left panels) and a sum-frequency (0.20 Hz) secondary wave (right panels). The upper and lower panels show the evolution of the amplitudes and biphase. Deep water primary wave amplitudes are 0.2 m.

Figure 3. Same model comparisons as shown in Figure 2 but with an obliquely propagating 0.12 Hz primary wave component (deep water incidence angle of 60°).

Figure 4. Secondary wave response (defined as the secondary wave amplitude normalized by the product of the primary wave amplitudes) in 4 m depth versus the deep water directional spreading angle of the primary wave components. The primary wave frequencies are 0.09 Hz, 0.11 Hz (upper panels) and 0.07 Hz, 0.13 Hz (lower panels). The lower frequency primary wave component is normally incident while the deep water incidence angle of the higher frequency primary wave varies between 0 and 60°. Difference and sum interactions are shown in the left and right panels, respectively. The beach slope is 0.01 and primary wave amplitudes in deep water are 0.2 m.

Figure 5. Secondary wave response in 4 m depth for primary waves with frequencies 0.08 and 0.12 Hz on a beach with slope 0.01. Upper and lower panels show results for deep water primary wave amplitudes of 0.1 and 0.4 m respectively (same format as Figure 4).

Figure 6. Secondary wave response in 4 m depth for 0.2 m amplitude primary waves with frequencies 0.08 and 0.12 Hz on beaches with slope 0.003 (upper panels) and 0.03 (lower panels) (same format as Figure 4).

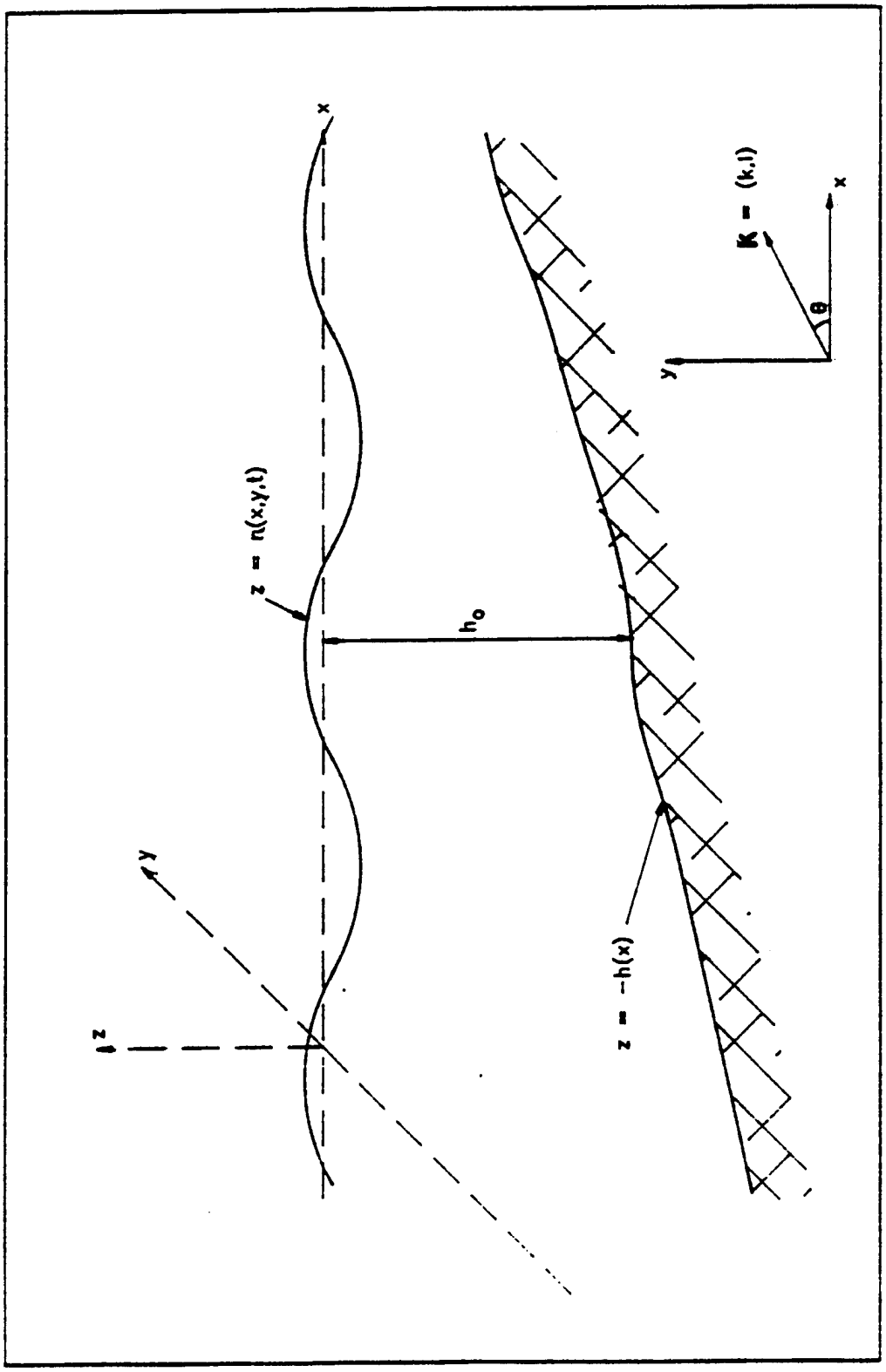

Figure 1.

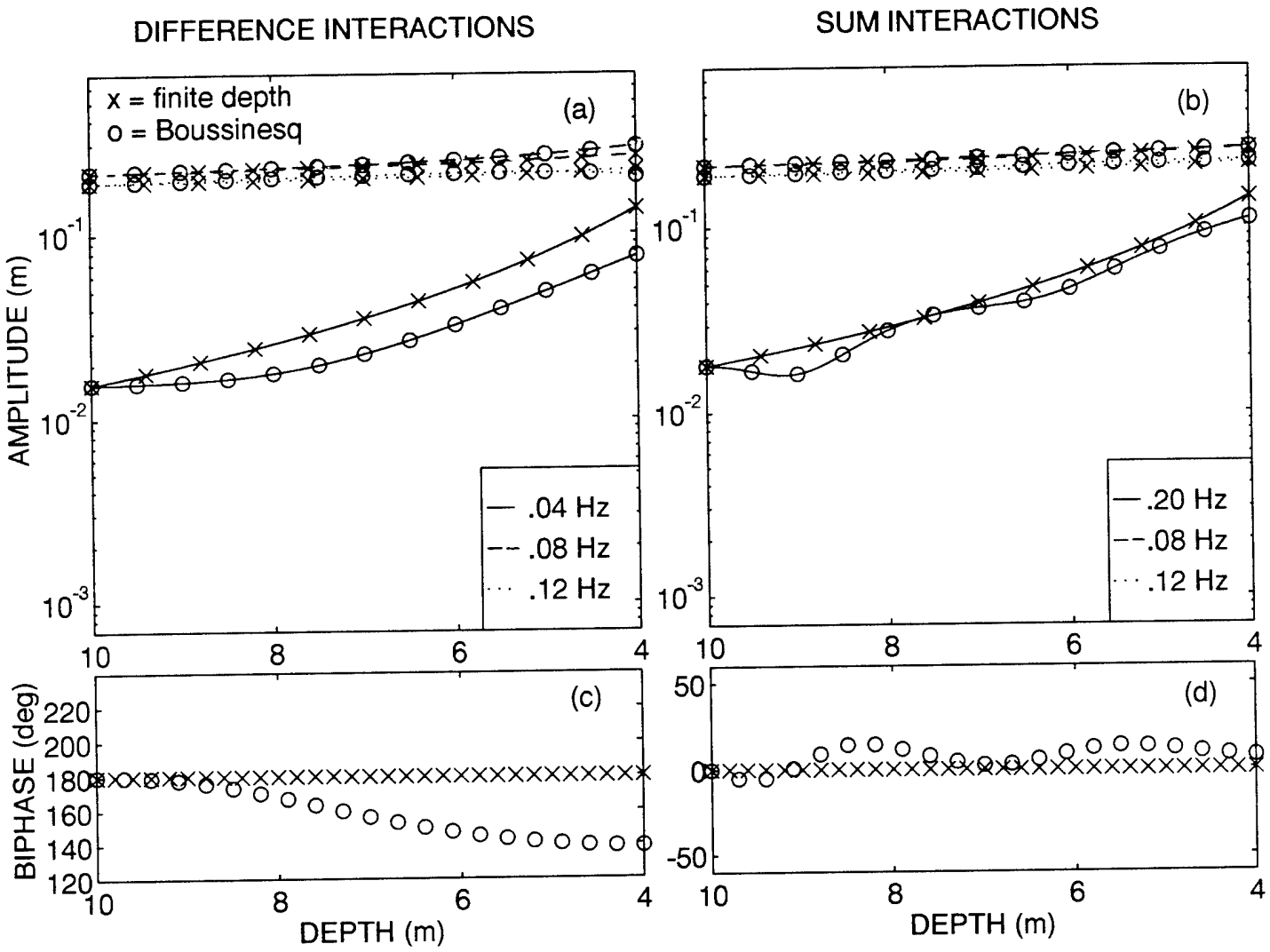
DIFFERENCE INTERACTIONS
SUM INTERACTIONS
x = finite depth
o = Boussinesq
(a)
(b)
(c)
(d)
AMPLITUDE (m)
BIPHASE (deg)
DEPTH (m)
DEPTH (m)
.04 Hz
.08 Hz
.12 Hz
.20 Hz
.08 Hz
.12 Hz

Figure 2

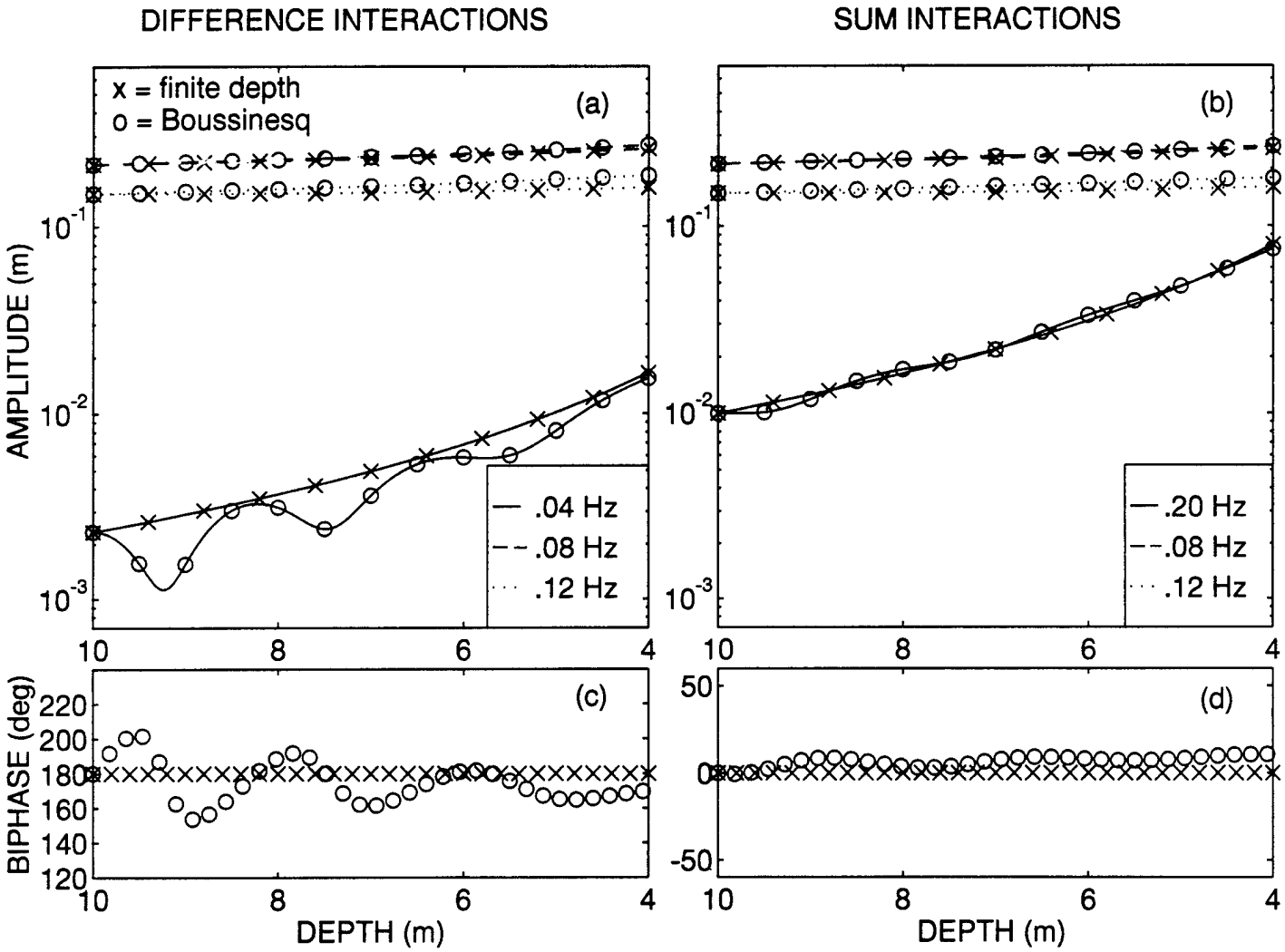
DIFFERENCE INTERACTIONS
SUM INTERACTIONS
x = finite depth
o = Boussinesq
(a)
(b)
(c)
(d)
AMPLITUDE (m)
BIPHASE (deg)
.04 Hz
.08 Hz
.12 Hz
.20 Hz
DEPTH (m)
DEPTH (m)

Figure 3

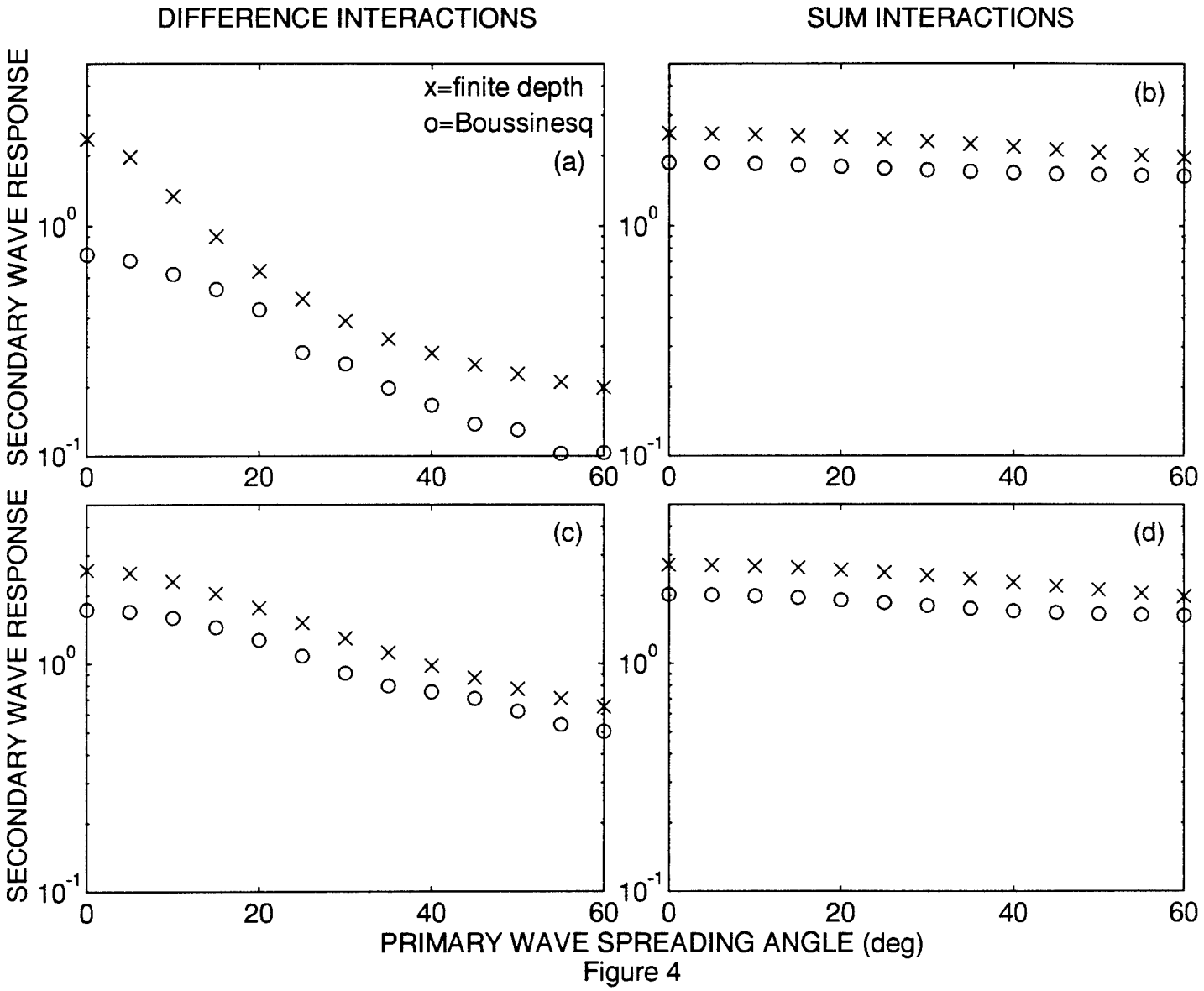
DIFFERENCE INTERACTIONS
SUM INTERACTIONS
x=finite depth
o=Boussinesq
(a)
(b)
(c)
(d)
SECONDARY WAVE RESPONSE
SECONDARY WAVE RESPONSE
10^0
10^{-1}
0
20
40
60
PRIMARY WAVE SPREADING ANGLE (deg)

Figure 4

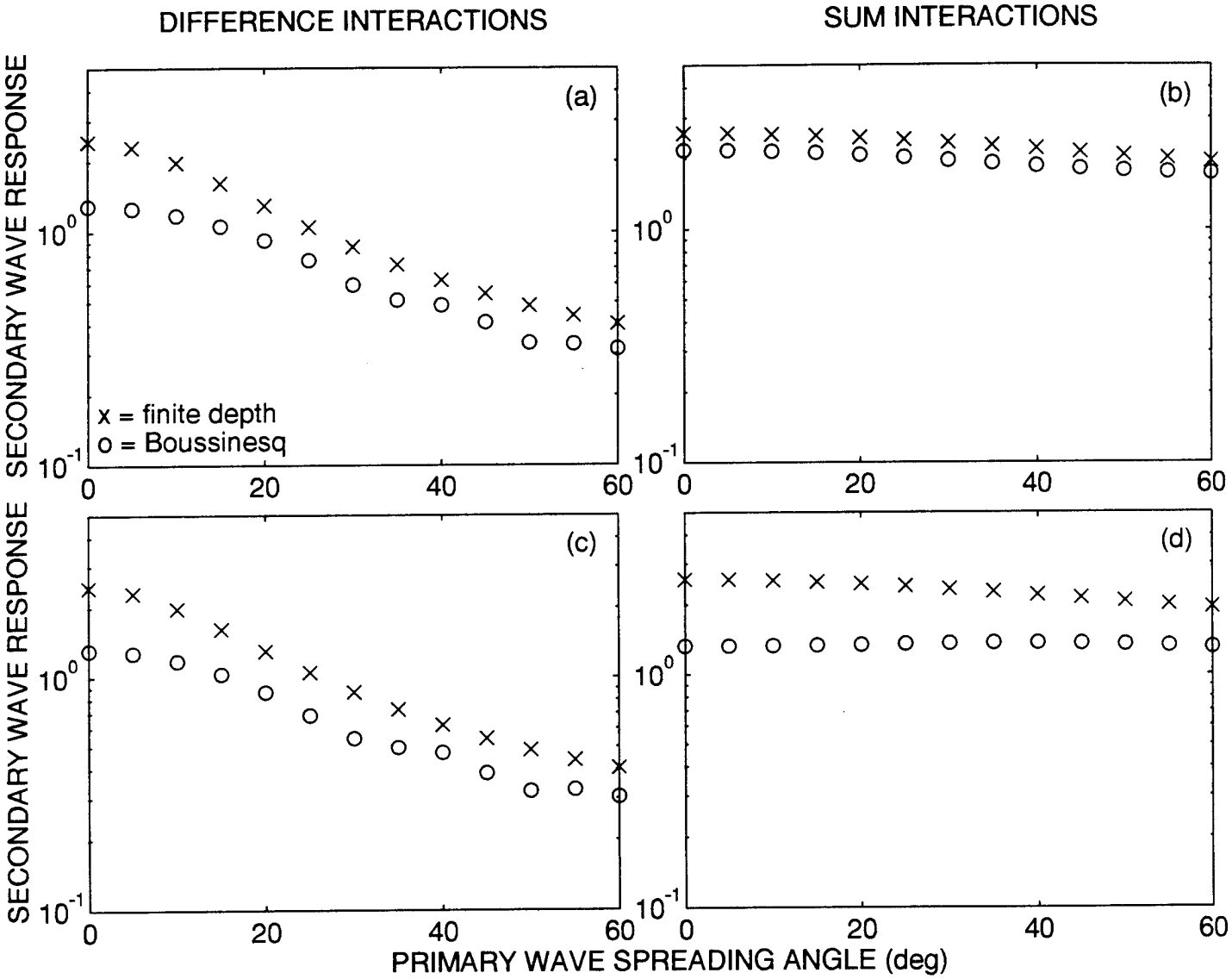
DIFFERENCE INTERACTIONS
SUM INTERACTIONS
(a)
(b)
(c)
(d)
x = finite depth
o = Boussinesq
SECONDARY WAVE RESPONSE
SECONDARY WAVE RESPONSE
10^0
10^{-1}
0
20
40
60
PRIMARY WAVE SPREADING ANGLE (deg)

Figure 5

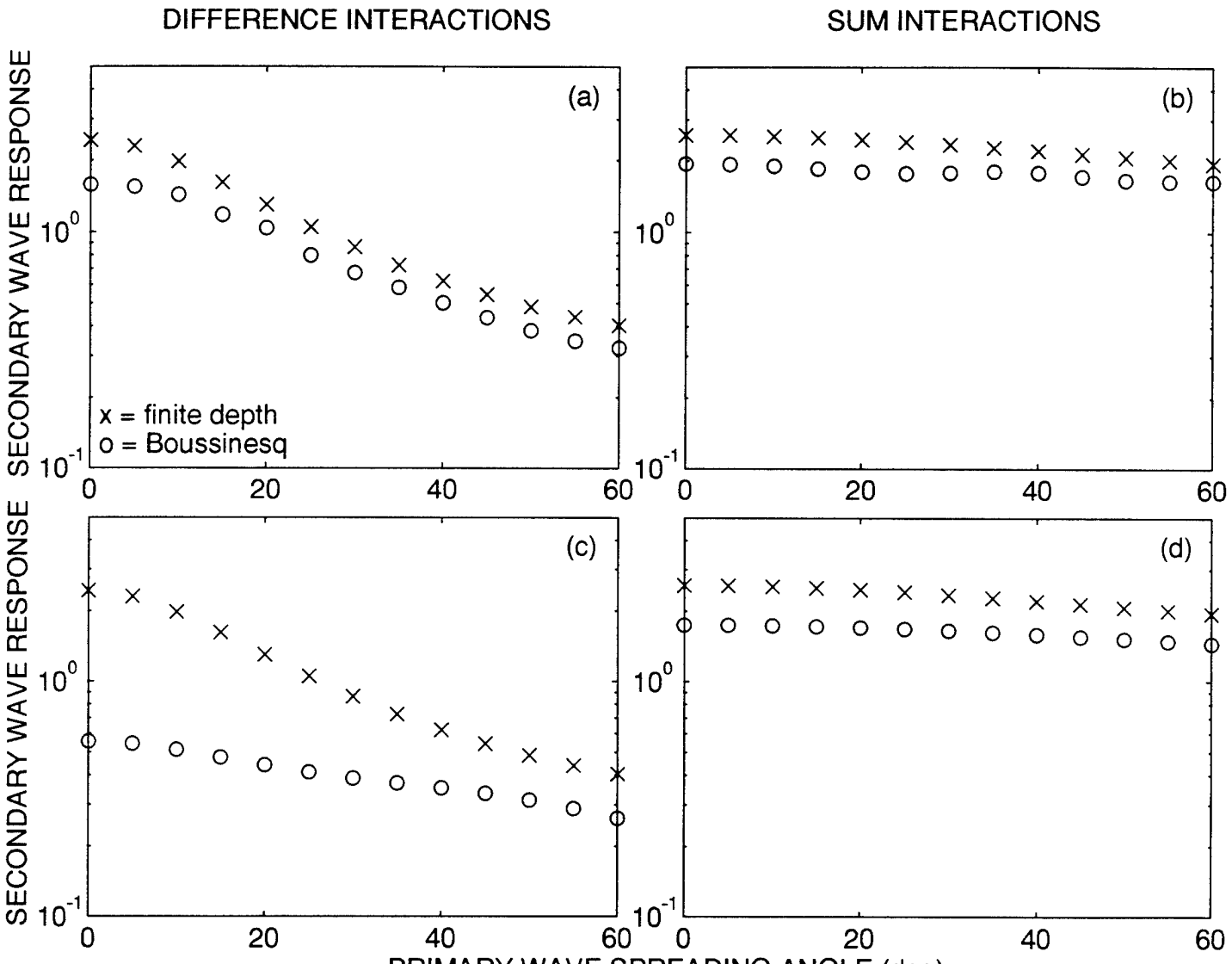
DIFFERENCE INTERACTIONS
SUM INTERACTIONS
SECONDARY WAVE RESPONSE
SECONDARY WAVE RESPONSE
(a)
(b)
(c)
(d)
x = finite depth
o = Boussinesq
10^0
10^{-1}
0
20
40
60
PRIMARY WAVE SPREADING ANGLE (deg)

Figure 6

LIST OF REFERENCES

Beach, R., and Sternberg, R., 1988, "Suspended Sediment in the Surf Zone: Response to Cross-shore Infragravity Motion", *Marine Geology* 80, 61-79.

Boussinesq, J., 1871, *Théorie Générale des Mouvements qui Sont Propagés dans un Canal Rectangulaire Horizontal*, C.R. Hebd. Séane, Acad. Sci., Paris 73, 256-260.

Elgar, S., Herbers, T.H.C., and Guza, R.T., 1994 "Reflection of Ocean Surface Gravity Waves from a Natural Beach", *J. Phys. Oceanogr.*, 24(7), 1503-1511.

Elgar, S. and Guza, R.T., 1985, "Observations of Bispectra of Shoaling Surface Gravity Waves," *J. Fluid Mech.*, 161, 425-448.

Elgar, S. and Guza, R.T., 1986, "Nonlinear Model Predictions of Bispectra of Shoaling Surface Gravity Waves", *J. Fluid Mech.*, 167, 1-18.

Freilich, M.H., and Guza, R.T., 1984, "Nonlinear Effects on Shoaling Surface Gravity Waves," *Phil. Trans. R. Soc. Land*, A311, 1-42.

Hasselmann, K., 1962, "On the Nonlinear Energy Transfer in a Gravity-Wave Spectrum, 1, General Theory," *J. Fluid Mech.*, 12, 481-500.

Herbers, T.H.C., and Guza, R.T., 1991, "Wind-Wave Nonlinearity Observed at the Sea Floor, Part 1, Forced Wave Energy," *J. Phys. Oceanogr.*, 21(12), 1740-1761.

_____ and _____, 1992, "Wind-Wave Nonlinearity Observed at the Sea Floor, Part 2, Wavenumbers and Third-Order Statistics," *J. Phys. Oceanogr.*, 22(5), 489-504.

_____ and _____, 1994, "Nonlinear Wave Interactions and High-Frequency Seafloor Pressure", *J. Geophys. Res.*, 99(c5), 10035-10048.

Herbers, T.H.C., Lowe, R.L., and Guza, R.T., 1992, "Field Observations of Orbital Velocities and Pressure in Weakly Nonlinear Surface Gravity Waves," *J. Fluid Mech.*, 245, 413-435.

Herbers, T.H.C., Elgar, S., and Guza, R.T., 1994, "Infragravity-Frequency (0.005-0.05 Hz) Motions on the Shelf, Part I, Forced Waves," *J. Phys. Oceanogr.*, 24(5), 917-927.

Herbers, T.H.C., Elgar, S., Guza, R.T., and O'Reilly, W.C., 1995a, "Infragravity-Frequency (0.005-0.05 Hz) Motions on the Shelf, Part II: Free Waves", *J. Phys. Oceanogr.*, in press.

Herbers, T.H.C., Elgar, S., and Guza, R.T., 1995b, "Generation and Propagation of Surf Beat", *J. Geophys. Res.*, submitted.

Holman, R.A., Huntley, D.A., and Bowen, A.J., 1978, "Infragravity Waves in Storm Conditions," *Proc. 16th Conf. on Coastal Engineering*, American Society of Civil Engineers, 268-284.

Liu, P.L.F., Yoon, S.B., and Kirby, J.T., 1985, "Nonlinear Refraction-Diffraction of Waves in Shallow Water," *J. Fluid Mech.*, 153, 185-201.

Longuet-Higgins, M.S. and Stewart, R.W., 1962, "Radiation Stress and Mass Transport in Gravity Waves, with Application to 'Surf Beats'," *J. Fluid Mech.*, 13, 481-504.

Mei, C.C. and LeMéhauté, B., 1966, "Note on the Equations of Long Waves over an Uneven Bottom," *J. Geophys. Res.*, 91(B7), 7343-7358.

Munk, W.H., 1949, "Surf Beats," *Trans. Amer. Geophys. Un.*, 30, 849-854.

Okihiro, M., Guza, R.T., and Seymour, R.J., "Bound Infragravity Waves", *J. Geophys. Res.*, 97, 11,453-11,469, 1992.

Peregrine, D.H., 1967, "Long Waves on a Beach," *J. Fluid Mech.*, 27, Part 4, 815-827.

Phillips, O.M., 1960, "On the Dynamics of Unsteady Gravity Waves of finite Amplitude, Part 1, The Elementary Interactions," *J. Fluid Mech.*, 9, 193-217.

Stokes, G.G., 1847, "On the Theory of Oscillatory Waves," *Trans. Camb. Phil. Soc.*, 8, 441-455.

Tucker, M.J., 1950, "Surf Beats: Sea Waves of 1 to 5 Minutes Period," *Proc. Roy. Soc.*, A202, 565-573.

Ursell, F., 1953, "The Long-Wave Paradox in the Theory of Gravity Waves," *Proc. Camb. Phil. Soc.*, 49, 685-694.

Wright, L.D., Guza, R.T., and Short, A.D., 1982, "Dynamics of a High-Energy Dissipative Surf Zone," *Mar. Geol.*, 45, 41-62.

INITIAL DISTRIBUTION LIST

1. Defense Technical Information Center 2
   Cameron Station
   Alexandria, VA 22304 - 6145

2. Library, Code 52 2
   Naval Postgraduate School
   Monterey CA 93943 - 5101

3. Professor T.H.C. Herbers, Code OC/He 8
   Department of Oceanography
   Naval Postgraduate School
   Monterey CA 93943 - 5121

4. Professor Frenzen, Code MA/Fr 1
   Department of Mathematics
   Naval Postgraduate School
   Monterey CA 93943 - 5121

5. Professor E.B. Thornton, Code OC/Tm 1
   Naval Postgraduate School
   Monterey CA 93943 - 5121

6. Professor T.C. Lippmann, Code OC/Li 1
   Department of Oceanography
   Naval Postgraduate School
   Monterey CA 93943 - 5121

7. Mark Burton 2
   1590 Harbor Blvd.
   Belmont, CA 94002